Biosensors and Bioelectronics 128 (2019) 52–60

Contents lists available at ScienceDirect

Biosensors and Bioelectronics

journal homepage: www.elsevier.com/locate/bios

Fully integrated digital microfluidics platform for automated immunoassay; A versatile tool for rapid, specific detection of a wide range of pathogens

Loïc Coudron[a,*], Martin B. McDonnell[a,b], Ian Munro[a], Daniel K. McCluskey[a], Ian D. Johnston[a], Christabel K.L. Tan[a], Mark C. Tracey[a]

[a] School of Engineering and Technology, University of Hertfordshire, College Lane, Hatfield AL10 9AB, United Kingdom
[b] Dstl Porton Down, Salisbury, Wiltshire SP4 0JQ, United Kingdom

ARTICLE INFO

Keywords:
Biodetection
Electrowetting
Digital microfluidics
Lab-on-a-chip
Immunoassay
Instrumentation

ABSTRACT

With the tangible threat posed by the release of chemical and biological warfare (CBW) agents, detection of airborne pathogens is a critical military and security concern. Recent air sampling techniques developed for biocollection take advantage of Electrowetting on Dielectric (EWOD) to recover material, producing highly concentrated droplet samples. Bespoke EWOD-based digital microfluidics platforms are very well suited to take full advantage of the microlitre concentrated droplet resulting from this recovery process. In this paper we present a free-standing, fully automated DMF platform for immunoassay. Using this system, we demonstrate the automated detection of four classes of CBW agent simulant biomolecules and organisms each representing credible threat agents. Taking advantage of the full magnetic separation process with antibody-bound microbeads, rapid and complete separation of specific target antigen can be achieved with minimal washing steps allowing for very rapid detection. Here, we report clear detection of four categories of antigens achieved with assay completion times of between six and ten minutes. Detection of HSA, Bacillus atrophaeus (BG spores), MS2 bacteriophage and Escherichia coli are demonstrated with estimated limit of detection of respectively 30 ng ml^{-1}, 4×10^4 cfu ml^{-1}, 10^6 pfu ml^{-1} and 2×10^7 cfu ml^{-1}. The fully-integrated portable platform described in this paper is highly compatible with the next generation of electrowetting-coupled air samplers and thus shows strong potential toward future in-field deployable biodetection systems and could have key implication in life-changing sectors such as healthcare, environment or food security.

1. Introduction

Dissemination of chemical and biological warfare (CBW) agents is unfortunately a tangible threat (Gooding, 2006). Defence and security agencies require technologies capable of addressing such threats by providing quick, efficient and specific detection of CBW agents (Franz et al., 1997; Gooding, 2006; Lane and Fauci, 2001; Lane et al., 2001; McDonnell, 1993; Naimushin et al., 2005), for which the aerosol route has been identified as a possible method of dissemination (Franz et al., 1997). Hence, detection of airborne pathogen is a critical military and security concern that also has key implication in sectors such as health and environment (Brunekreef and Holgate, 2002; Garrett et al., 1998; Rainer et al., 2001; Sarıca et al., 2002; Tuet et al., 2017) or food (Mahlein et al., 2012; West and Kimber, 2015). Lab-on-a-chip systems have been developed to tackle the challenges in sample collection and address the potentially very low concentration of airborne pathogen (Fronczek and Yoon, 2015). In the last ten years, electrowetting-on-dielectric (EWOD) based digital microfluidics (DMF) (Abdelgawad and Wheeler, 2009; Jebrail et al., 2012; Mugele and Baret, 2005; Nelson and Kim, 2012; Pollack et al., 2000), used in conjunction with various air-sampling techniques, has been envisioned as a powerful tool to produce in-droplet highly concentrated sample from airborne collected material (Jönsson-Niedziółka et al., 2011; Zhao and Cho, 2006; Zhao et al., 2008). More recently, a personal air sampler using EWOD based DMF as a way to increase the sampling concentration rate has been demonstrated (Foat et al., 2016). This technique produces highly concentrated droplet samples that can be transferred into a bespoke bio-detector. The use of immunoassay as a detection technique appears particularly relevant in this context. Whilst being relatively simple compared to other methods such as DNA hybridization assays (Diamandis, 1990) they can offer fast, high specificity detection of a large range of target species (Diamandis, 1990; Wild, 2013). Heterogeneous immunoassays, which rely on specific binding of a target antigen in solution to a solid-bound antibody (e.g. wall, surface or suspended particles), are popular

* Corresponding author.
E-mail address: l.coudron@herts.ac.uk (L. Coudron).

https://doi.org/10.1016/j.bios.2018.12.014
Received 8 June 2018; Received in revised form 29 November 2018; Accepted 11 December 2018
Available online 18 December 2018
0956-5663/ Crown Copyright © 2018 Published by Elsevier B.V. All rights reserved.

amongst immunoassay techniques because of their good sensitivity and high specificity (Wild, 2013). In their simplest form, they consist of the separation of a target antigen from other material in solution by extracting the solid-bound antibody-antigen complex. The target separated in this way can be detected, typically using another antibody, conjugated with an optical label, such as a fluorophore, or an enzyme that will trigger a reaction (e.g. colour change, chemiluminescence or chemifluorescence) at the detection substrate.

To take full advantage of the highly concentrated small volume samples resulting from the collection process, it is desirable to use them undiluted in their microlitre-droplets form. EWOD based DMF appears very well suited: in addition to an obviously very straight-forward integration with other EWOD based systems such as the one presented by Foat et al. (2016), DMF carries the promise of a possible paradigm shift in micro-volume bioassays by allowing complex manipulation of discrete microlitre-scale droplets (Abdelgawad and Wheeler, 2009). In the last decade, a number of these systems have been developed to serve as a platform for DNA or antibody based assays using magnetic particles as solid support for the separation of target material (Kokalj et al., 2015). The use of magnetic particles is particularly interesting, especially for use in DMF systems because they can be transported within a fluid droplet and be trapped or released by respectively engaging or disengaging magnets at a specific magnetic separation site. While DNA assays benefit from a higher sensitivity and specificity, immunoassays are capable of addressing a large range of targets, including for example toxins, which makes them suitable for application in a versatile biodetection system.

Sista et al. (2008) reported the first generation of DMF platform for magnetic microparticles-based heterogeneous immunoassays. This system, operating in oil filler, achieved separation of the target by a serial dilution-based process, consisting of the repetition of three steps comprising the immobilization of the magnetic particles followed by the dilution of the suspension with a droplet of fresh buffer before splitting the droplet into two droplets, one containing the magnetic particles and the other the particle-free excess solution. Employing this principle the system performed on-chip non-competitive immunoassays for insulin and interleukin-6. Employing a similar kind of immunoassay, an optimised version of this system was used to perform completely automated detection of cardio troponin I (cTn1) on whole blood (Sista et al., 2008). Since then, pursuing the promise of precise, fast and sequential low-volume automation, a number of immunoassay applications have been developed on DMF platforms (Choi et al., 2013; Dixon et al., 2016; Fobel et al., 2014; Ng et al., 2012, 2015a; Vergauwe et al., 2011).

Actuating biomaterial-laden droplets, as required in a DMF bioassay, can cause biomaterial and objects present in the droplet to be deposited and/or adsorbed at the surface of the actuation chip. This phenomenon, referred to as biofouling, can cause severe droplet actuation impairment and, eventually, device malfunction (Au et al., 2011; Luk et al., 2008). In order to reduce the biofouling rate, some DMF platforms operate in oil (Sista et al., 2008; Vergauwe et al., 2011). Whilst showing good performance in terms of biofouling prevention, the use of oil filler is not ideal within the scope of the application presented above due to limited connectivity and field-transportability that the use of oil implies (Ng et al., 2012): a special packaging is required for oil containment and connection with other air-filled DMF devices, such as Foat et al.'s (2016), may be compromised. There is also the risk of trace molecules within the oil infiltrating the droplet thus interfering with the droplet's chemistry (Au et al., 2011; Yoon and Garrell, 2003) or small molecules exfiltrating from the droplet into the medium (Ng et al., 2015b), which could jeopardise the sensitivity of detection. The Wheeler Group presented an alternative to oil-filled systems by using non-ionic surfactant to reduce biomolecule deposition (Au et al., 2011; Luk et al., 2008). Using this approach, they developed a fully automated in-air DMF platform for immunoassays (Choi et al., 2013; Dixon et al., 2016; Fobel et al., 2014; Ng et al., 2012, 2015a). Building on the technique first demonstrated on a single plate EWOD device by Fouillet et al. (2008), the Wheeler Group's system features efficient extraction of magnetic particles from droplet supernatant (Choi et al., 2013; Dixon et al., 2016; Fobel et al., 2014; Ng et al., 2012, 2015a). This allows complete specific separation of the target using a reduced number of washing steps. With their open-access platform DropBot (Fobel et al., 2013), the Wheeler Group demonstrated detection of a number of biomarkers (thyroid stimulating hormone (Choi et al., 2013; Ng et al., 2012), 17β-estradiol (Ng et al., 2012), Rubella IgG (Dixon et al., 2016; Fobel et al., 2014; Ng et al., 2015a) and Rubella IgM (Ng et al., 2015a). Recently, the Wheeler Group has demonstrated in-field diagnostics against measles and rubella immunoglobulin G (IgG) in remote northwestern Kenya's population using a fully integrated version of their DMF immunoassay platform (Ng et al., 2018).

In the context of medical diagnostics that the platforms above are addressing, the patient has already been exposed to pathogens or other threat agents and has produced biomarkers that will be detected. In current state of the art DMF platform for immunoassay, only indirect detection of pathogens, i.e. detection of clinical biomarkers resulting from the infection process, has been performed. However, when detecting from an airborne sample, the pathogen itself must be directly detected. In addition, to offer a sufficiently rapid response to such pathogen, the detection should ideally occur in the field, close to the threat location. Hence the detection platform should be easily man-transportable, preferably oil-free, self-contained, i.e. not requiring external hardware and fully automated. Implementing all these features, the platform developed by the Wheeler Group (Ng et al., 2018) and the system described here, developed in parallel, based on defence specifications, are arguably by far, the two most advanced, potentially deployable, DMF biodetection systems.

In this paper, for the first time on a EWOD chip, using a bespoke, free-standing, fully automated DMF platform for immunoassay, we demonstrate the rapid detection of four classes of CBW agent simulant biomolecules and organisms representing threat agents or other pathogens, namely: proteins (toxins), vegetative bacteria, bacterial spores and viruses. The design and realisation of the different components constituting the integrated, completely self-contained DMF platform, including the high voltage waveform generator and drive electronics will be discussed in the experimental section. The performance of this system is assessed against fully automated detection of human serum albumin (HSA, a globular protein), *Escherichia coli* (*E. coli*, a vegetative bacteria), *Bacillus atrophaeus* (BG, a bacterial spore) and MS2 (a bacteriophage virus). It is expected that the system described here, when coupled with an in-droplet collection strategy, has the potential to address future aspirations for efficient detection of (airborne) pathogens.

2. Experimental section

2.1. Material and method

HEPES (4-(2-Hydroxyethyl)piperazine-1-ethanesulfonic acid, N-(2-Hydroxyethyl)piperazine-N′-(2-ethanesulfonic acid) hemi-sodium salt pH 7.5 (Sigma Aldrich H9897) was used to make up the main assay running buffer. The HEPES salt was diluted into DI water to form a 100 mM HEPES solution at a pH of 7.5 and Tween™ 80 (Surfact-Amps™ Detergent Solution, ThermoFisher Scientific 28328) was added to a concentration of 0.01% v/v.

The magnetic microparticles employed in this study are functionalised Pierce™ NHS-Activated Magnetic Beads (ThermoFisher Scientific 88826). The beads have a mean diameter $d = 1\,\mu m$ and a magnetic susceptibility $\chi \approx 0.1$ (S.I.) estimated in accordance with the value of magnetic susceptibility of magnetite (Fe_3O_4) that can be found elsewhere (Kelland, 1973).

The beads were derivatised with antibody using the commercially available Pierce™ Direct Magnetic IP/Co-IP Kit following the manufacturer's instructions. Before use, the antibody coated beads were

Table 1
Antigens and antibodies used in the EWOD assay development and testing. Unless stated otherwise, materials listed in this table were provided by the Defence Science and Technology Laboratory (Dstl, UK). The following abbreviations are used: Rb for rabbit, cfu for colony forming units and pfu for plaque forming units.

Antigen	Antigen's stock concentration	Capture antibody	Detection antibody
HSA (Abcam, UK)	10.3 mg/ml	Anti-Human Serum Albumin [15C7] (Abcam ab10241)	Anti-Human Serum Albumin [1A9] (HRP) (Abcam ab24438)
B. atrophaeus (BG) spores	9.5×10^8 cfu ml^{-1}	Rb anti-BG polyclonal	Biotinylated Rb anti-BG polyclonal
E. coli MRE 162	3×10^9 cfu ml^{-1}	Rb anti-*E. coli* MRE 162 polyclonal	Biotinylated Rb anti-*E. coli* MRE 162 polyclonal
MS2 virus	1×10^8 pfu ml^{-1}	Goat anti-MS2 polyclonal	Biotinylated Rb anti-MS2 polyclonal

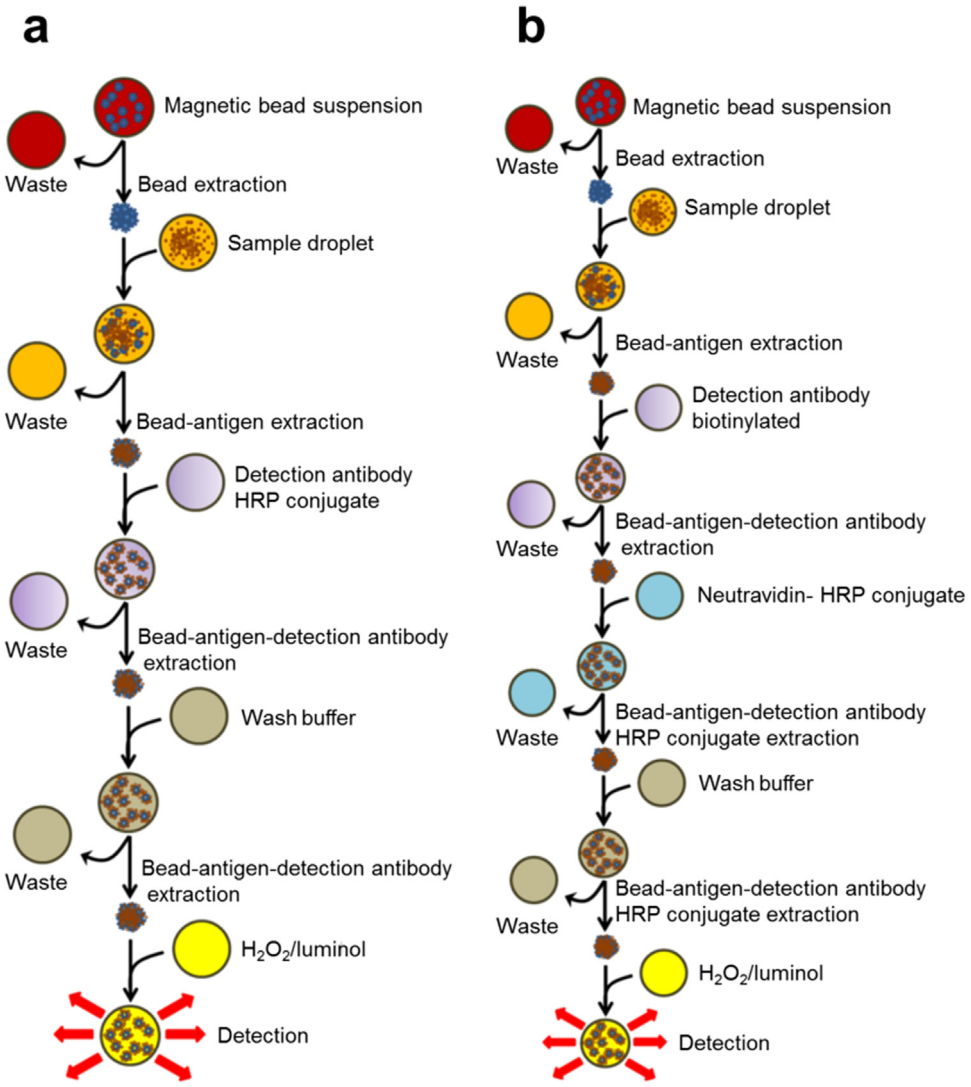

Fig. 1. Schematic diagram of the EWOD immunoassays: (a) four-extractions assay sequence using a detection antibody-HRP conjugate, (b) five extractions assay sequence using biotinylated detection antibody.

blocked by suspension overnight in Blocker™ Casein (1% w/v) in PBS buffer (TFS 37582, ThermoFisher Scientific, UK) at a concentration of 4 mg/ml. Using a permanent magnet to separate the beads from supernatant, the beads were then washed three times in buffer before suspending them in running buffer at the test concentration of 2.5 mg/ml.

The antigens as well as the capture (attached to the microbeads) and detection antibodies used in this study, and their respective provenance are listed in the Table 1.

The biodetection assay (Fig. 1) used in this study involves the selective capture of antigen by antibody coated magnetic beads followed by the addition of a secondary detection antibody leading ultimately to the measureable emission of light from a chemiluminescent reaction. The process utilises a sequence of stepwise manipulations dependent on the effective extraction, resuspension and mixing of the magnetic beads within 2.5 µl droplets. Light generation is triggered by the reaction between the enzyme horseradish peroxidase (HRP) present on the beads (depending on the quantity of captured antigen) and a luminol substrate (SuperSignal™ ELISA Femto Substrate, TFS 37075, ThermoFisher Scientific, UK) brought to the beads at the end of the process in the form of a droplet used to resuspend and mix the beads. The luminescent droplet is subsequently moved by EWOD to the photodetector for light collection. The enzyme is attached directly (HSA assay) or indirectly (BG, *E. coli* and MS2 assays) via a NeutrAvidin®-biotin (Pierce™ High

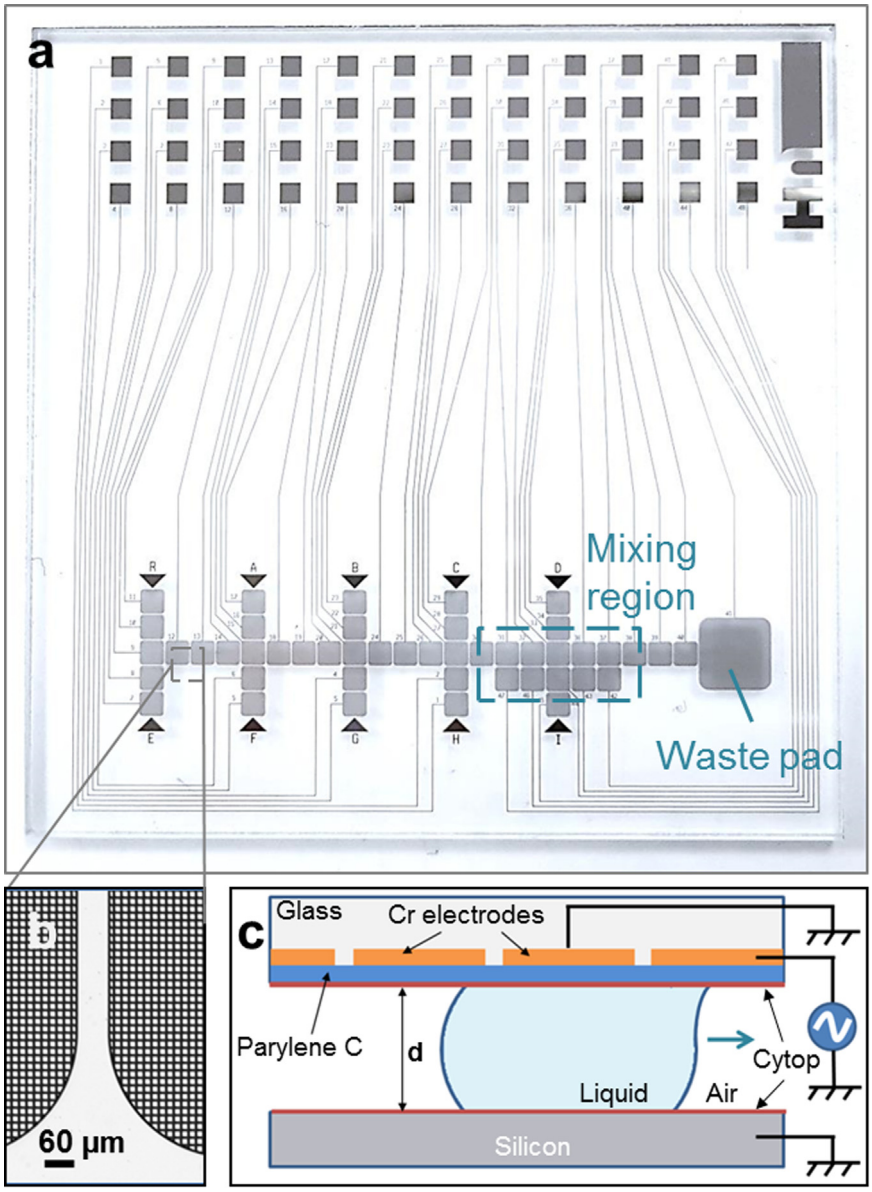

Fig. 2. Overview of the EWOD chip setup. (a) EWOD actuation plate. (b) pad, magnification x20. (c) schematic drawing of the parallel-plate EWOD chip in operation.

Sensitivity NeutrAvidin™- horseradish peroxidase conjugate, TFS 31030, ThermoFisher Scientific, UK) or streptavidin-poly-HRP (Pierce™ Streptavidin Poly-HRP, TFS 21140, ThemoFisher Scientific, UK) linkage to the detection antibody. The basic assay sequence with the use of a detection antibody-HRP conjugate is summarised in Fig. 1a. The use of a biotinylated detection antibody instead of an antibody-HRP conjugate requires an additional on-chip step using a droplet containing NeutrAvidin®-HRP or streptavidin-poly-HRP conjugate (Fig. 1b). In some experiments, using biotinylated detection antibody, the antibody and the conjugate are premixed off-chip to save the extra on-chip step.

2.2. The design and fabrication of the EWOD chip

The central component of the DMF platform is the EWOD chip (Fig. 2). The EWOD actuation plate (Fig. 2a) comprises 47 electrodes each independently addressed by 48 channel electronics (described in the next section). Each electrode is $1.7 \times 1.7\,mm^2$ for typical droplet volumes ranging from 1.5 µl to 3 µl. To provide semi-transparency, the pads are filled by a grid design (Fig. 2b). A rectangular pattern composed of eight electrodes constitutes the mixing region of the plate. A larger $5 \times 5\,mm^2$ pad is used as waste pad for separated supernatant. The EWOD chip operates using the common parallel-plate configuration (Fig. 2c) (Latip et al., 2017). In this configuration, the droplet is sandwiched between the hydrophobic surfaces of the actuation plate and a conductive, grounded cover plate both separated by a precisely defined gap. In the present embodiment, the gap (d) is 500 µm, set using specified thickness plastic spacers. In our operating configuration, the cover plate is located at the bottom of the EWOD chip while the droplet is actuated by locally applied electric field via the actuation plate at the top.

A commercially available chrome (Cr) mask fabrication service (Compugraphics, Scotland) was used to manufacture the electrode array on the glass plate (Cr thickness typically is 1000 Å) according to our design. The plates were precisely cut to size using a SYJ-400 precision CNC Dicing/Cutting Saw (MTI Corp, USA). The cut Cr/glass plates were coated with a 6 µm thick Parylene-C layer as dielectric layer. The Parylene-C was deposited following the Gorham process (Gorham, 1967) using 7.4 g of DPX-C dimer in a SCS Parylene Deposition System 2010 'Labcoater 2' (Specialty Coating System, USA). A layer of Cytop® was deposited on top of the dielectric layer to provide

Fig. 3. The digital microfluidics platform. (a) Overview of the all-integrated platform in operation; the dark faraday cage, in which the EWOD operation, the magnetic separation and the detection are performed, allows a minimal electromagnetic interference; the platform is connected to a computer running the bespoke software interface controlling droplet operation. The approximated dimensions of the unit are 26 × 30 × 30 cm^3. (b) The platform with the chamber opened and its rotating stage in running position (magnet at the bottom). (c) The platform with rotating stage in droplet loading position (magnet on top). (d) The platform in droplet loading position with the lid (magnet attached) removed and the loading deck on. (e) Sprung-loaded connector (pogo pins) for electrical connection with the EWOD plate. (f) Integrated electronics: the top board comprises the wave generator and the bottom board encompasses the control electronics. (g) The photodetector board comprising pre-filters and shielding case. (h) Manual pipetting of droplet through the droplet loading deck. (i) EWOD chip comprising the loaded droplets, the green arrow points to the detection site.

hydrophobicity to the EWOD surface. The Cytop® was spin-coated in a Süss Microtec 'Labspin' spin-coater (SÜSS MicroTec AG, Germany) at 1500 rpm for 30 s and the plates were then baked at 140 °C for 30 min. The cover plate is made of a 500 µm thick, 4-in. silicon wafer (p-type, < 100 > , 1–10 Ω cm, Pi Kem Ltd), on which a Cytop® layer was deposited according to the process described above.

2.3. DMF platform

The DMF bioassay platform (Fig. 3) integrates all the necessary components required to perform a complete chemiluminescent immunoassay. The platform includes a dark Faraday cage chamber to isolate it from stray light and to avoid electromagnetic interference affecting the detection electronics. This allows the chemiluminescent reaction between the enzyme horseradish peroxidase (HRP) and the luminol substrate to be monitored by a photodiode (S9270 photodiode, Hamamatsu, Japan). The fully integrated platform performs automated manipulation and transportation of magnetic micro-particles suspended in bio-material laden droplets. Droplets are ideal vessels for such solid micro-objects; in contrast to continuous flow in microchannels where transportation of suspended solid objects is problematic due to obstruction of the flow by the objects, there is no risk of such clogging in droplet-based DMF. The platform allows fully-automated immunoprecipitation involving the separation of the magnetic solid phase from the supernatant using an automated permanent magnet. The platform, controlled with a bespoke software interface, is fully-operated via an USB-connected computer and a UK main power-socket (Fig. 3a).

To remove any potential negative influence of gravity on the magnetic separation process, the platform operates with the vertically movable N42 cylindrical magnet (25 mm diameter and 10 mm height) located at the bottom of the silicon cover plate (Fig. 3b). The magnet, embedded in a 3D-printed protective case can be automatically moved up and down for either magnetic separation or re-suspension of the magnetic particles. A standard commercial off-the-shelf Arduino Uno controller board with an additional L298H bridge motor controller IC (STMicroelectronics, Switzerland) is used to control the magnetic actuator by driving a small DC gear motor (Pololu, USA) that is connected to the driveshaft of the magnetic actuator assembly. Opto-switches detect when the motor has driven the magnet to either the retracted (magnet off) or extended (magnet on) position. A binary signal from the EWOD droplet transport modules determines whether the magnet should be extended or retracted. Additionally, the Arduino uses a Pulse Width Modulated signal to control the speed of the motor and thus gradually slow it down before contacting the silicon plate.

The magnet assembly is mechanically aligned with the EWOD chip via precise positioning of the magnet with respect to the droplet at the prescribed separation site. The mechanical assembly contains a rotary stage allowing 180° rotation to alter the platform from its running position to its droplet loading position (Fig. 3c & d). The magnet assembly is fixed on the lid, which can be unclamped and removed to free the

silicon cover plate. With the cover plate removed (Fig. 3d), the EWOD actuation plate can be slotted into place (or removed) and connected to the telescopic sprung loaded probes (otherwise commonly known as pogo pins) to establish electrical contact with the drive electronics (Fig. 3e).

The EWOD drive electronics (Fig. 3f) consists of a stack of two PCBs, both powered from a PC via a USB cable, which are respectively responsible for the high voltage drive of the system on one board and for PC communication, channel switching and capacitive feedback measurement system on the other.

The high voltage drive for the system is controlled by a Microchip 18F45K22 microcontroller. The microcontroller contains an 8 bit sine wave lookup table, the values of which are continuously iterated though, and output to an R-2R resistor ladder to produce a 1 kHz analog sine wave. This signal is then filtered and amplified to be used as the EWOD actuation signal on the assay plate. The operating RMS (root mean square) voltage ranges from 0 V to 225 V and is varied by the micro-controller altering the value of a digital potentiometer determining pre-amplification.

The lower communication board is responsible for the high voltage signal addressing as well as droplet feedback. The board is controlled by an 18F67K22 microcontroller. The board can control 48 independent drive channels. Each channel consists of 2 high voltage MOSFET switches (ASSR4118 photo MOSFET SSR), chosen for their low leakage current, high voltage capability and small form factor to allow on one electrode channel to both control and sensing of a droplet. These switches are arranged such that each channel can be connected to the high voltage AC source for droplet actuation, or to the analog to digital converter (A/D) of the microcontroller (including a MOSFET allowing ground connection) for droplet sensing. The droplet sensing method is based on capacitive feedback but unlike the common feedback systems encountered in DMF, it doesn't rely on a ring oscillator. Instead the droplet sensing system is based on charge accumulation during current injection. Feedback at rest and during droplet actuation is possible by simply measuring with the microcontroller A/D input after the microcontroller has injected a known current for a fixed time period using the Charge Time Measurement Unit of the microcontroller.

A droplet actuation operation sequence would typically consist of the following events: The PC sends a command to the microcontroller declaring what drive voltage is required, followed by a command declaring which channels should be switched on and for what duration. The microcontroller then connects the required drive channels to the high voltage drive, enables the high voltage drive for the specified time, then disables the high voltage drive. Disabling the drive turns off all sine-wave generation rather than just disconnecting the drive so as to reduce possible interference sources during the charge measurement phase (droplet sensing). Once the drive is disabled all the switches are simultaneously closed for 20 ms to dissipate any residual charge. After all residual charge has been removed the switches are then set to connect the channels to the A/D for droplet sensing. The software compares the measured charge level of the droplet destination pad with the previous known droplet's location. By examining the difference in these values it can be determined whether the droplet has successfully moved.

The optical detection module (Fig. 3g) is based around a Hamamatsu S9270 photodiode with an integrated preamplifier. The S9270 was chosen for its large 10 mm × 10 mm collection area to maximise light collection without collection optics and integrated trans-impedance amplifier to minimise noise. The amplifier has a built in feedback resistor of 1 GΩ and a built in feedback capacitor of 5 pf. This

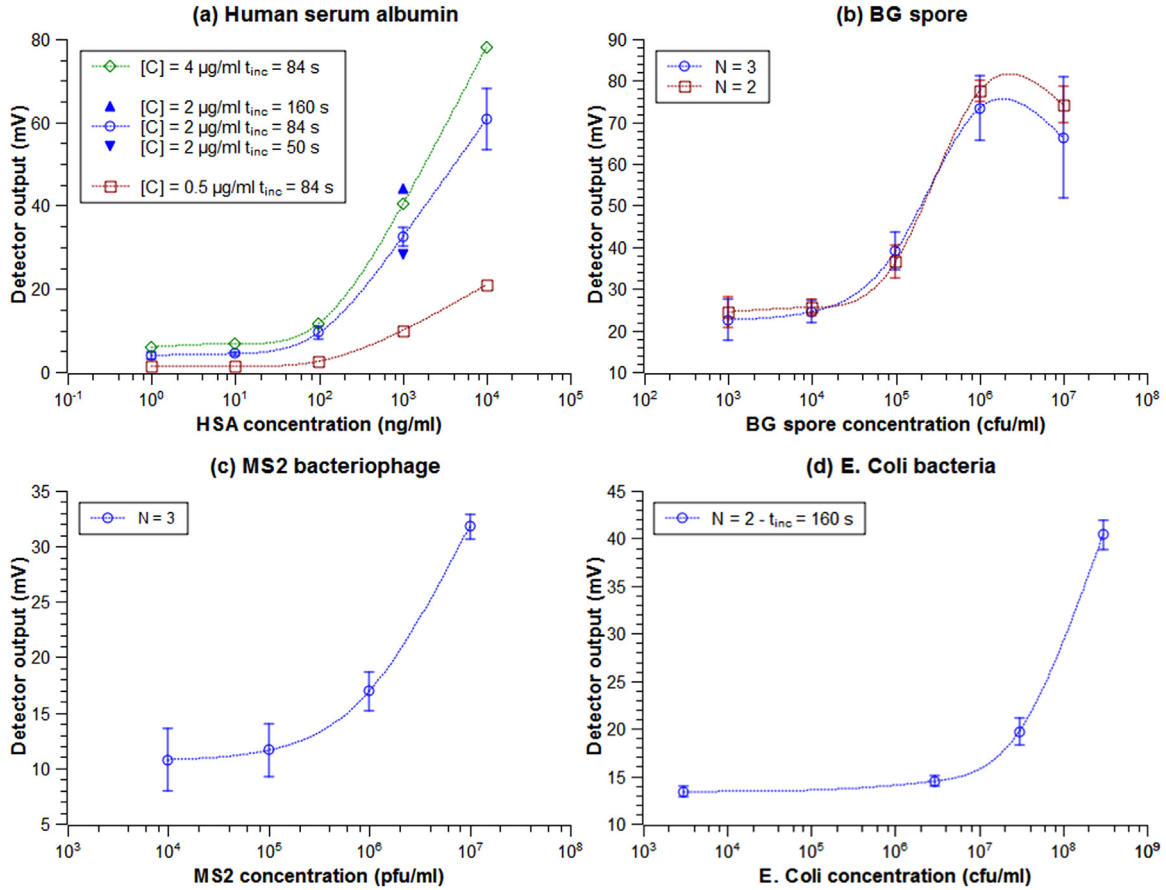

Fig. 4. EWOD immunoassay result, unless indicated otherwise, the incubation time (t_{inc}) is 84 s (a) Human serum albumin. (b) BG spore. (c) MS2 bacteriophage. (d) *E. coli* bacteria.

means that 1 nA of photodiode current will produce and output voltage of 1 V with a bandwidth of 32 Hz. In order to minimise noise magnitude, with the module having an output noise voltage of 9.7 μVrms/Hz, a 1 nf capacitor was placed in parallel with the built in 5 pf reducing the bandwidth to 0.15 Hz and thus reducing the noise at source. To reduce other possible noise and interference sources, the signal was fed directly into an Analog Devices AD7799 low noise 24 bit A/D. The A/D also has a 90 dB 50 Hz filter when sampling at 16.7 Hz and a noise floor of 1.45uV rms. The A/D uses a Linear Technology LTC6655 precision voltage reference. The A/D is interfaced to PIC18F14K22 microcontroller which is connected to the PC via and FT232R USB to serial interface. Further reduction in EMI sources was achieved by careful PCB design including placing all analog components in a screened 'can'.

The EWOD chip is aligned with the photodetector (Fig. 3h & i) allowing for a precise detection site for the luminescent droplet at the centre of the collection area for maximum light collection. Sample and reagents are brought onto the EWOD plate using bespoke loading deck (Fig. 3h) for precise manual pipetting of the 2.5 μl droplets onto their initial delivery pad. Up to ten droplets can be loaded this way to allow for up to nine separation steps assay.

3. Results

When aiming at rapid, specific detection, reducing the number of assay steps is a desirable outcome. For this purpose, using a technique reported elsewhere (Ng et al., 2012), the full extraction of the magnetic beads from the droplet is a very efficient way to achieve the complete specific separation of the target with minimum dilution and/or washing steps. The detailed mechanism and theory of the magnetic full extraction process (Appendix A) and a video of the magnetic extraction step can be found online as Supplementary material.

Supplementary material related to this article can be found online at doi:10.1016/j.bios.2018.12.014.

Whilst, an increase of the voltage directly increases the actuation force, hence facilitating magnetic extraction, it also participates in increasing the biofouling rate (Latip et al., 2017; Yoon and Garrell, 2003). Accordingly, based on a series of preliminary experiments described in Appendix B (available online as Supplementary material), 105 V_{rms} was selected as the operating voltage for the DMF assay with a couple of exceptions: firstly, the minimal reliable actuation for the luminol:H_2O_2 droplet was found to be 120 V_{rms} and secondly, a higher voltage of 165 V_{rms} was used to produce a higher force during the magnetic separation process. All of these voltages are implemented in the automated sequence used to perform the fully automatic immunoassay.

Taking advantage of the full magnetic separation process with antibody-bound microbeads and using minimal washing steps, very rapid detection is achieved. Here, we report clear detection of four categories of antigens (see Fig. 4), achieved with assay times as short as six minutes and no longer than ten minutes.

Detection of HSA (Fig. 4a) involved the use of an anti-HSA detection antibody directly functionalised with HRP. Three different concentrations of this conjugate were used to provide information of the dependency of the specific detection and non-specific background signals on that variable (0.5, 2.0 and 4.0 μg ml^{-1}). All these measurements were made with an incubation time of the antibody capture beads with the sample of 84 s, allowing a rapid total assay time of 6 min. During the incubation period, and as for all other assays presented here, the droplet was kept moving following a mixing pattern in the mixing region of the EWOD chip.

A conjugate concentration of 2.0 μg ml^{-1} was selected for a more detailed study with standard deviations (n = 3) obtained for all antigen concentrations measured. An estimated limit of detection (LoD) of approximately 30 ng ml^{-1} is obtained. A single experiment with an antigen concentration of 10^3 ng ml^{-1} with an extended sample incubation of 160 s showed a 36% increase in signal with no increase in the non-specific background signal. This suggests a potential reduction of the LoD to approximately 18 ng ml^{-1} while maintaining a rapid assay time of 7.4 min.

For the detection of BG spores (Fig. 4b) a biotinylated detection antibody combined with a NeutrAvidin®-HRP conjugate was used. To simplify the assay, the biotinylated detection antibody and conjugate were premixed to reduce the number of assay steps. Both were at final concentrations of 1 μg ml^{-1}. The assay shows a relatively high background due to non-specific binding of the HRP conjugate. Although clear positive responses are obtained at concentrations above 10^4 cfu ml^{-1}, the relatively high standard deviations obtained from the data indicate a limit of detection of approximately 4×10^4 cfu ml^{-1}. From the plot it appears that there may be a 'hook effect' at concentrations above 10^6 cfu ml^{-1}, but this cannot be confirmed due to the high standard deviations in the experimental data.

The MS2 bacteriophage is employed to demonstrate detection of a viral antigen (Fig. 4c). As with the BG assay, the biotinylated rabbit anti-MS2 antibody was pre-mixed with the Neutravidin-HRP conjugate, both at a concentration of 1 μg ml^{-1}. The antigen incubation time was 84 s. A clear positive response at concentrations above 10^5 pfu ml^{-1} is obtained, however the relatively high SDs indicate a limit of detection of approximately 10^6 pfu ml^{-1}, a very promising result nonetheless considering the short assay time of 6 min.

Finally, detection of a vegetative bacterial antigen is shown using *E. coli* (Fig. 4d). In contrast to the BG and MS2 assays, the biotinylated rabbit anti-*E. coli* antibody (3.6 μg ml^{-1}) was not pre-mixed with the enzyme conjugate. In order to enhance the response signal Neutravidin HRP conjugate was replaced with streptavidin poly-HRP at a concentration of 1 μg ml^{-1}. The antigen incubation time was 168 s. Two wash steps were included prior to luminol addition to minimise background noise. The fairly high LoD of 2×10^7 cfu ml^{-1} is balanced by the low sample volume needed and the short assay time (albeit longer than for the other species) of ten minutes.

4. Discussion

The use of a DMF platform for bioassays combines the advantage of low volume samples and short assay times whilst retaining, and in some cases improving upon, typical LoD performance characteristics of most common biosensing methods (Ivnitski et al., 1999; McBride et al., 2003; Rowe et al., 1999; Speight et al., 1997), which are often considerably more time consuming and/or require several orders of magnitude larger sample volume. Whilst the versatility of the technique is proven, one caveat concerns the fairly high LoD obtained for the vegetative bacteria representative (E. coli) resulting from the limitations of the available antibodies for that particular antigen. Improvements in the detection performance should be obtained by the selection of higher affinity antibodies or by the selection of antibodies for which target epitopes are present at higher densities on the surface of the micro-organism.

In general, detection performance could be improved by increasing the detection sensitivity while reducing the chemiluminescent background caused by the non-specific binding (NSB) of the antibody-HRP complex to the magnetic beads. Using higher affinity antibodies will increase the desired reaction signal in absolute terms. However, even with an increased sensitivity in detection, the NSB is the main current limiting factor for the LoD. Further investigation to reduce the NSB may be involving the selection of a new blocking agent for the beads as an alternative to the casein protein blocker employed in this study and a modified formulation of the buffer and surfactant.

Disregarding the LoD issue, the detection sensitivity could be further improved via several routes. In the current configuration, prior to reaching the photodetector surface, the optical signal is attenuated by the semi-transparency of the grid Cr electrode of the EWOD structure. Accordingly, it is anticipated that using fully transparent electrodes could significantly increase the optical signal and hence sensitivity. It would also be possible to increase the photodetector's sensitivity. A very obvious way to achieve this would be to replace the present photodiode

by one of higher sensitivity such as a Silicon PhotoMultiplier (SiPM) device.

A question regarding the use of immunoassays is raised by the Fig. 4b where the large uncertainties of data point for the highest concentration of the analyte can be attributed to a slow degradation of reagents during the course of a day's tests. The results obtained by plotting only the data obtained using fresh solutions (N = 2) are also shown on the same graph. Whilst the comparison between the N = 2 and N = 3 plots seems to indicate that the impact of reagent degradation on the LoD is very marginal, general future investigation concerning the stability of antibody solutions when used in the field would be valuable.

It should be noted that, whist important, the limit of detection of the biosensor isn't the only factor on the bio-detection process that determines the likelihood of detecting very low concentrations of airborne pathogen. The probability for a target to be detected is a function of the sensor's LoD as well the concentration of the collected sample introduced into the detector. Hence, it is essential to maximise the concentration of the sample resulting from the collection stage of the bio-detection chain. We propose that our detection technique should be used in conjunction with a DMF-based air sampler, such as that presented by Foat et al. (2016), which produces highly concentrated droplet samples. Such a sampling technique relies on continuous sampling over a period of time prior to a concentration step using EWOD based DMF to transfer the material into a liquid droplet. Although, for such systems in general, real-time detection of threat aerosols should be the ultimate aim, this is not currently achievable due to the requirement for very rapid but highly specific measurement of the very low agent concentrations in a widely fluctuating biological background combined with a resulting high reagent burden when operating in the field. A more realistic approach is for detection to be achieved sufficiently early to allow for affected personnel to receive appropriate medical treatment. This could be achieved by using continuous collection of aerosol combined with rapid analysis of the resulting sample at user selected intervals or triggered, for example, by a reagentless continuously monitoring aerosol counter (Kaye and Hirst, 2015).

To further explore the significance of the results presented in this paper, a brief hypothetical case-study involving detection of airborne *Bacillus anthracis* using our detector coupled to the DMF-based air sampler presented by Foat et al. (2016) is conducted here. Whilst hypothetical, the study employs experimental results from both this paper and Foat et al.'s (2016). The following assumptions are made:

- BG, employed in this study, is routinely used as a simulant for *B. anthracis* by the defence community (Ho and Duncan, 2005). It is therefore assumed that the values for collection efficiency of BG and the LoD of BG respectively estimated in the study from Foat et al. (2016) and in this paper would be similar to the one of *B. anthracis* and will therefore be used interchangeably in the projection.
- The respiratory minute volume of a moderately active person is assumed to be V_R = 20 l/min (Altman and Dittmer, 1971)
- The retention ratio of inhaled organisms is considered to be 100%.

From the perspective of CBW protection, *B. anthracis,* responsible for the Anthrax disease, is arguably the primary bio warfare threat (Gutting et al., 2012; Primmerman, 2000). Although not precisely known for humans, the median infective dose ID50 (dose that will infect 50% of the exposed population) of *B. anthracis* can be estimated at around 10,000 spores based on the values found in the literature (Goel, 2015; Primmerman, 2000; Toth et al., 2013). The infection time (time for ID50 to be inhaled, t_{ID50}) to the minimum sampling time (time for the sampler to achieve the LoD, t_{LoD}) ratio can be estimated as follow (Eq. (1)):

$$\frac{t_{ID50}}{t_{LoD}} = \frac{ID50 \bullet R_C}{LoD \bullet V_R} \quad (1)$$

with R_c being the sampler's concentration rate as defined by the product of the system's collection efficiency and the flow rate divided by the sample's volume. The collection efficiency of BG reported by Foat et al. (2016) using the ESP-EWOD system ranges from 1.3% to 5.4%. For a 2.5 µl volume output such as introduced to the detector of the present study, R_c ranges from 1.4 10^5 min^{-1} to 5.4 10^5 min^{-1}. Using the DMF immunoassay platform presented in this paper, detection of BG can be achieved with a LoD of 4 10^4 cfu/ml. Accordingly, the ratio of infection time to the minimum sampling time can be estimated between 1.9 and 7.4, which means that a detectable sample can be collected 1.9 times to 7.4 times faster than for a subject exposed to inhale the ID50, hence allowing detection to potentially occur prior to infection. At the very least, employing DMF-based detection could allow threats to be identified shortly after exposure thereby enabling rapid response including medical countermeasures.

Exploring some plausible scenario of malicious airborne dissemination (Ho and Duncan, 2005; Reshetin and Regens, 2003), the concentration of aerosolised *B. anthracis* can vary from low, 0.007 cfu/ml to very high, 160 cfu/ml. At the latter concentration, one human breath cycle will be sufficient to inhale more than 10 times the ID50. In this case, early detection will allow timely treatment but will be unlikely to prevent infection that could occur as soon as the subject is exposed. However, at the lower concentration of 0.007 cfu/ml, using our very simplistic assumption, it would take approximately 70 min for a subject exposed to inhale the ID50. In this kind of situation, using our detector coupled to the DMF-based air sampler, the minimum time for the DMF-based sampler to collect a sample of detectable concentration (i.e. the LoD) ranges between 10 min and 38 min. Thus the short DMF assay time of 6–10 min reported here, would allow pre-infective detection to be included within the range of possibilities.

5. Conclusions

A bespoke digital microfluidic immunoassay platform has been demonstrated, which addresses the limitations of aerosol detection of CBW agents. For the first time on an EWOD chip, rapid, efficient and specific detection of four common types of representative pathogen - simulant biomolecules and organisms (proteins, vegetative bacteria, bacterial spores and viruses) has been achieved.

Rapid, fully automated detection of *E. coli*, BG, MS2 and HSA have been demonstrated as a proof of concept for versatile biodetection.

In recent years, EWOD-based air sampling systems achieving high concentration rate have been developed. These systems exploit small volume droplets to produce highly concentrated sample in-droplet from collected aerosol material. The fully-integrated portable platform described in this paper is highly compatible with this next generation of electrowetting-coupled air samplers and thus shows strong potential toward future in-field deployable bio detection systems. The development of such technology could impact a wide range of disciplines with life-changing repercussion including food security (crop pathogen monitoring) and healthcare (point of care diagnostics).

With this paper, we hope to demonstrate that DMF is a very promising technique to address the crucial bio-detection challenges posed by early detection of weaponised aerosols. With the concepts presented here and thanks to the democratisation of DMF systems, strongly underpinned by a decade of research and exemplified by the recent foundation of DMF systems solution providers such as Sci-Bots and GaudiLabs, we anticipate that continuous improvement of the state-of-the-art of DMF systems will be crucial to the development of the next generation of in-field bio-detectors.

Acknowledgements

We are very grateful to our colleagues from the Microfluidic and Microengineering Research Group for their contribution to the mechanical design and we wish to acknowledge Dstl Porton Down's long

standing support for, and collaboration with, our digital microfluidics and biodetection research.

Conflicts of interest

There are no conflicts to declare.

Declaration of interests

None.

Appendix A. Supporting information

Supplementary data associated with this article can be found in the online version at https://doi.org/10.1016/j.bios.2018.12.014.

References

Abdelgawad, M., Wheeler, A.R., 2009. The digital revolution: a new paradigm for microfluidics. Adv. Mater. 21 (8), 920–925.

Altman, P., Dittmer, D., 1971. Biological Handbooks: Respiration and Circulation. Federation of American Societies for Experimental Biology, Bethesda, MD.

Au, S.H., Kumar, P., Wheeler, A.R., 2011. A new angle on pluronic additives: advancing droplets and understanding in digital microfluidics. Langmuir 27 (13), 8586–8594.

Brunekreef, B., Holgate, S.T., 2002. Air pollution and health. Lancet 360 (9341), 1233–1242.

Choi, K., Ng, A.H., Fobel, R., Chang-Yen, D.A., Yarnell, L.E., Pearson, E.L., Oleksak, C.M., Fischer, A.T., Luoma, R.P., Robinson, J.M., 2013. Automated digital microfluidic platform for magnetic-particle-based immunoassays with optimization by design of experiments. Anal. Chem. 85 (20), 9638–9646.

Diamandis, E.P., 1990. Analytical methodology for immunoassays and DNA hybridization assays—current status and selected systems—critical review. Clin. Chim. Acta 194 (1), 19–50.

Dixon, C., Ng, A.H., Fobel, R., Miltenburg, M.B., Wheeler, A.R., 2016. An inkjet printed, roll-coated digital microfluidic device for inexpensive, miniaturized diagnostic assays. Lab Chip 16 (23), 4560–4568.

Foat, T., Sellors, W., Walker, M., Rachwal, P., Jones, J., Despeyroux, D., Coudron, L., Munro, I., McCluskey, D., Tan, C., 2016. A prototype personal aerosol sampler based on electrostatic precipitation and electrowetting-on-dielectric actuation of droplets. J. Aerosol Sci. 95, 43–53.

Fobel, R., Fobel, C., Wheeler, A.R., 2013. DropBot: an open-source digital microfluidic control system with precise control of electrostatic driving force and instantaneous drop velocity measurement. Appl. Phys. Lett. 102 (19), 193513.

Fobel, R., Kirby, A.E., Ng, A.H., Farnood, R.R., Wheeler, A.R., 2014. Paper microfluidics goes digital. Adv. Mater. 26 (18), 2838–2843.

Fouillet, Y., Jary, D., Chabrol, C., Claustre, P., Peponnet, C., 2008. Digital microfluidic design and optimization of classic and new fluidic functions for lab on a chip systems. Microfluid. Nanofluidics 4 (3), 159–165.

Franz, D.R., Jahrling, P.B., Friedlander, A.M., McClain, D.J., Hoover, D.L., Bryne, W.R., Pavlin, J.A., Christopher, G.W., Eitzen, E.M., 1997. Clinical recognition and management of patients exposed to biological warfare agents. Jama 278 (5), 399–411.

Fronczek, C.F., Yoon, J.-Y., 2015. Biosensors for monitoring airborne pathogens. J. Lab. Autom. 20 (4), 390–410.

Garrett, M., Rayment, P., Hooper, M., Abramson, M., Hooper, B., 1998. Indoor airborne fungal spores, house dampness and associations with environmental factors and respiratory health in children. Clin. Exp. Allergy 28 (4), 459–467.

Goel, A.K., 2015. Anthrax: a disease of biowarfare and public health importance. World J. Clin. Cases: WJCC 3 (1), 20.

Gooding, J.J., 2006. Biosensor technology for detecting biological warfare agents: recent progress and future trends. Anal. Chim. Acta 559 (2), 137–151.

Gorham, W.F., 1967. Para-xylylene polymers. US patent 3,342,754.

Gutting, B., Nichols, T.L., Channel, S.R., Gearhart, J.M., Andrews, G.A., Berger, A.E., Mackie, R.S., Watson, B.J., Taft, S.C., Overheim, K.A., 2012. Inhalational anthrax (Ames aerosol) in naïve and vaccinated New Zealand rabbits: characterizing the spread of bacteria from lung deposition to bacteremia. Front. Cell. Infect. Microbiol. 2, 87.

Ho, J., Duncan, S., 2005. Estimating aerosol hazards from an anthrax letter. J. Aerosol Sci. 36 (5–6), 701–719.

Ivnitski, D., Abdel-Hamid, I., Atanasov, P., Wilkins, E., 1999. Biosensors for detection of pathogenic bacteria. Biosens. Bioelectron. 14 (7), 599–624.

Jebrail, M.J., Bartsch, M.S., Patel, K.D., 2012. Digital microfluidics: a versatile tool for applications in chemistry, biology and medicine. Lab Chip 12 (14), 2452–2463.

Jönsson-Niedziółka, M., Lapierre, F., Coffinier, Y., Parry, S., Zoueshtiagh, F., Foat, T., Thomy, V., Boukherroub, R., 2011. EWOD driven cleaning of bioparticles on hydrophobic and superhydrophobic surfaces. Lab Chip 11 (3), 490–496.

Kaye, P.H., Hirst, E., 2015. Second generation low-cost particle counter. U.S. Patent No. 9, 116,121. 25 Aug. 2015.

Kelland, D., 1973. High gradient magnetic separation applied to mineral beneficiation. IEEE Trans. Magn. 9 (3), 307–310.

Kokalj, T., Perez-Ruiz, E., Lammertyn, J., 2015. Building bio-assays with magnetic particles on a digital microfluidic platform. New Biotechnol. 32 (5), 485–503.

Lane, H.C., Fauci, A.S., 2001. Bioterrorism on the home front: a new challenge for American medicine. Jama 286 (20), 2595–2597.

Lane, H.C., La Montagne, J., Fauci, A.S., 2001. Bioterrorism: a clear and present danger. Nat. Med. 7 (12), 1271–1273.

Latip, E.N.A., Coudron, L., McDonnell, M.B., Johnston, I.D., McCluskey, D.K., Day, R., Tracey, M.C., 2017. Protein droplet actuation on superhydrophobic surfaces: a new approach toward anti-biofouling electrowetting systems. RSC Adv. 7 (78), 49633–49648.

Luk, V.N., Mo, G.C., Wheeler, A.R., 2008. Pluronic additives: a solution to sticky problems in digital microfluidics. Langmuir 24 (12), 6382–6389.

Mahlein, A.-K., Oerke, E.-C., Steiner, U., Dehne, H.-W., 2012. Recent advances in sensing plant diseases for precision crop protection. Eur. J. Plant Pathol. 133 (1), 197–209.

McBride, M.T., Gammon, S., Pitesky, M., O'Brien, T.W., Smith, T., Aldrich, J., Langlois, R.G., Colston, B., Venkateswaran, K.S., 2003. Multiplexed liquid arrays for simultaneous detection of simulants of biological warfare agents. Anal. Chem. 75 (8), 1924–1930.

McDonnell, M., 1993. Biosensors in the Detection of Biological Agents. Uses of Immobilized Biological Compounds. Springer, pp. 369–375.

Mugele, F., Baret, J.-C., 2005. Electrowetting: from basics to applications. J. Phys.: Condens. Matter 17 (28), R705.

Naimushin, A.N., Spinelli, C.B., Soelberg, S.D., Mann, T., Stevens, R.C., Chinowsky, T., Kauffman, P., Yee, S., Furlong, C.E., 2005. Airborne analyte detection with an aircraft-adapted surface plasmon resonance sensor system. Sens. Actuators B: Chem. 104 (2), 237–248.

Nelson, W.C., Kim, C.-J.C., 2012. Droplet actuation by electrowetting-on-dielectric (EWOD): a review. J. Adhes. Sci. Technol. 26 (12–17), 1747–1771.

Ng, A.H., Choi, K., Luoma, R.P., Robinson, J.M., Wheeler, A.R., 2012. Digital microfluidic magnetic separation for particle-based immunoassays. Anal. Chem. 84 (20), 8805–8812.

Ng, A.H., Fobel, R., Fobel, C., Lamanna, J., Rackus, D.G., Summers, A., Dixon, C., Dryden, M.D., Lam, C., Ho, M., 2018. A digital microfluidic system for serological immunoassays in remote settings. Sci. Transl. Med. 10 (438), eaar6076.

Ng, A.H., Lee, M., Choi, K., Fischer, A.T., Robinson, J.M., Wheeler, A.R., 2015a. Digital microfluidic platform for the detection of rubella infection and immunity: a proof of concept. Clin. Chem. 61 (2), 420–429.

Ng, A.H., Li, B.B., Chamberlain, M.D., Wheeler, A.R., 2015b. Digital microfluidic cell culture. Annu. Rev. Biomed. Eng. 17, 91–112.

Pollack, M.G., Fair, R.B., Shenderov, A.D., 2000. Electrowetting-based actuation of liquid droplets for microfluidic applications. Appl. Phys. Lett. 77 (11), 1725–1726.

Primmerman, C.A., 2000. Detection of biological agents. Linc. Lab. J. 12 (1), 3–32.

Rainer, J., Peintner, U., Pöder, R., 2001. Biodiversity and concentration of airborne fungi in a hospital environment. Mycopathologia 149 (2), 87–97.

Reshetin, V.P., Regens, J.L., 2003. Simulation modeling of anthrax spore dispersion in a bioterrorism incident. Risk Anal.: Int. J. 23 (6), 1135–1145.

Rowe, C.A., Tender, L.M., Feldstein, M.J., Golden, J.P., Scruggs, S.B., MacCraith, B.D., Cras, J.J., Ligler, F.S., 1999. Array biosensor for simultaneous identification of bacterial, viral, and protein analytes. Anal. Chem. 71 (17), 3846–3852.

Sarıca, S., Asan, A., Otkun, M.T., Ture, M., 2002. Monitoring indoor airborne fungi and bacteria in the different areas of Trakya University Hospital, Edirne, Turkey. Indoor Built Environ. 11 (5), 285–292.

Sista, R., Hua, Z., Thwar, P., Sudarsan, A., Srinivasan, V., Eckhardt, A., Pollack, M., Pamula, V., 2008. Development of a digital microfluidic platform for point of care testing. Lab Chip 8 (12), 2091–2104.

Speight, S., Hallis, B., Bennett, A., Benbough, J., 1997. Enzyme-linked immunosorbent assay for the detection of airborne microorganisms used in biotechnology. J. Aerosol Sci. 28 (3), 483–492.

Toth, D.J., Gundlapalli, A.V., Schell, W.A., Bulmahn, K., Walton, T.E., Woods, C.W., Coghill, C., Gallegos, F., Samore, M.H., Adler, F.R., 2013. Quantitative models of the dose-response and time course of inhalational anthrax in humans. PLoS Pathog. 9 (8), e1003555.

Tuet, W.Y., Chen, Y., Fok, S., Champion, J.A., Ng, N.L., 2017. Inflammatory responses to secondary organic aerosols (SOA) generated from biogenic and anthropogenic precursors. Atmos. Chem. Phys. 17 (18), 11423–11440.

Vergauwe, N., Witters, D., Ceyssens, F., Vermeir, S., Verbruggen, B., Puers, R., Lammertyn, J., 2011. A versatile electrowetting-based digital microfluidic platform for quantitative homogeneous and heterogeneous bio-assays. J. Micromech. Microeng. 21 (5), 054026.

West, J., Kimber, R., 2015. Innovations in air sampling to detect plant pathogens. Ann. Appl. Biol. 166 (1), 4–17.

Wild, D., 2013. The Immunoassay Handbook: Theory and Applications of Ligand Binding, ELISA and Related Techniques. Newnes.

Yoon, J.-Y., Garrell, R.L., 2003. Preventing biomolecular adsorption in electrowetting-based biofluidic chips. Anal. Chem. 75 (19), 5097–5102.

Zhao, Y., Cho, S.K., 2006. Microparticle sampling by electrowetting-actuated droplet sweeping. Lab Chip 6 (1), 137–144.

Zhao, Y., Chung, S.K., Yi, U.-C., Cho, S.K., 2008. Droplet manipulation and microparticle sampling on perforated microfilter membranes. J. Micromech. Microeng. 18 (2), 025030.